# First Observation of $B_s^0 \to J/\psi\eta$ and $B_s^0 \to J/\psi\eta'$

J. Li,[46] I. Adachi,[11] H. Aihara,[54] K. Arinstein,[2] D. M. Asner,[42] V. Aulchenko,[2] T. Aushev,[18] A. M. Bakich,[48] V. Bhardwaj,[33] B. Bhuyan,[12] M. Bischofberger,[33] A. Bondar,[2] A. Bozek,[37] M. Bračko,[28,19] O. Brovchenko,[21] T. E. Browder,[10] M.-C. Chang,[5] A. Chen,[34] P. Chen,[36] B. G. Cheon,[9] R. Chistov,[18] K. Cho,[22] S.-K. Choi,[8] Y. Choi,[47] J. Dalseno,[29,50] Z. Doležal,[3] A. Drutskoy,[18] S. Eidelman,[2] S. Esen,[4] J. E. Fast,[42] V. Gaur,[49] A. Garmash,[2] Y. M. Goh,[9] J. Haba,[11] T. Hara,[11] K. Hayasaka,[32] H. Hayashii,[33] Y. Horii,[32] Y. Hoshi,[52] W.-S. Hou,[36] Y. B. Hsiung,[36] H. J. Hyun,[24] T. Iijima,[32,31] K. Inami,[31] A. Ishikawa,[53] R. Itoh,[11] M. Iwabuchi,[60] Y. Iwasaki,[11] T. Iwashita,[33] T. Julius,[30] J. H. Kang,[60] P. Kapusta,[37] N. Katayama,[11] T. Kawasaki,[39] H. J. Kim,[24] H. O. Kim,[24] J. B. Kim,[23] K. T. Kim,[23] M. J. Kim,[24] Y. J. Kim,[22] K. Kinoshita,[4] B. R. Ko,[23] N. Kobayashi,[55] P. Kodyš,[3] S. Korpar,[28,19] P. Križan,[26,19] P. Krokovny,[2] T. Kuhr,[21] R. Kumar,[43] A. Kuzmin,[2] Y.-J. Kwon,[60] J. S. Lange,[6] M. J. Lee,[46] S.-H. Lee,[23] Y. Li,[58] J. Libby,[13] C. Liu,[45] Y. Liu,[36] Z. Q. Liu,[15] D. Liventsev,[18] R. Louvot,[25] D. Matvienko,[2] S. McOnie,[48] Y. Miyazaki,[31] R. Mizuk,[18] G. B. Mohanty,[49] A. Moll,[29,50] T. Mori,[31] N. Muramatsu,[44] I. Nakamura,[11] E. Nakano,[41] M. Nakao,[11] H. Nakazawa,[34] Z. Natkaniec,[37] S. Nishida,[11] K. Nishimura,[10] O. Nitoh,[57] S. Ogawa,[51] T. Ohshima,[31] S. Okuno,[20] S. L. Olsen,[46,10] W. Ostrowicz,[37] G. Pakhlova,[18] C. W. Park,[47] H. K. Park,[24] K. S. Park,[47] T. K. Pedlar,[27] T. Peng,[45] R. Pestotnik,[19] M. Petrič,[19] L. E. Piilonen,[58] M. Prim,[21] M. Röhrken,[21] S. Ryu,[46] H. Sahoo,[10] K. Sakai,[11] Y. Sakai,[11] T. Sanuki,[53] Y. Sato,[53] O. Schneider,[25] C. Schwanda,[16] A. J. Schwartz,[4] K. Senyo,[59] O. Seon,[31] M. E. Sevior,[30] M. Shapkin,[17] V. Shebalin,[2] C. P. Shen,[31] T.-A. Shibata,[55] J.-G. Shiu,[36] F. Simon,[29,50] P. Smerkol,[19] Y.-S. Sohn,[60] A. Sokolov,[17] S. Stanič,[40] M. Starič,[19] M. Sumihama,[7] T. Sumiyoshi,[56] S. Tanaka,[11] G. Tatishvili,[42] Y. Teramoto,[41] K. Trabelsi,[11] M. Uchida,[55] S. Uehara,[11] Y. Unno,[9] S. Uno,[11] P. Urquijo,[1] Y. Usov,[2] G. Varner,[10] K. E. Varvell,[48] V. Vorobyev,[2] A. Vossen,[14] C. H. Wang,[35] P. Wang,[15] M. Watanabe,[39] Y. Watanabe,[20] J. Wicht,[11] K. M. Williams,[58] E. Won,[23] Y. Yamashita,[38] C. Z. Yuan,[15] Z. P. Zhang,[45] V. Zhilich,[2] and A. Zupanc[21]

(Belle Collaboration)

[1]*University of Bonn, Bonn*
[2]*Budker Institute of Nuclear Physics SB RAS and Novosibirsk State University, Novosibirsk 630090*
[3]*Faculty of Mathematics and Physics, Charles University, Prague*
[4]*University of Cincinnati, Cincinnati, Ohio 45221*
[5]*Department of Physics, Fu Jen Catholic University, Taipei*
[6]*Justus-Liebig-Universität Gießen, Gießen*
[7]*Gifu University, Gifu*
[8]*Gyeongsang National University, Chinju*
[9]*Hanyang University, Seoul*
[10]*University of Hawaii, Honolulu, Hawaii 96822*
[11]*High Energy Accelerator Research Organization (KEK), Tsukuba*
[12]*Indian Institute of Technology Guwahati, Guwahati*
[13]*Indian Institute of Technology Madras, Madras*
[14]*Indiana University, Bloomington, Indiana 47408*
[15]*Institute of High Energy Physics, Chinese Academy of Sciences, Beijing*
[16]*Institute of High Energy Physics, Vienna*
[17]*Institute of High Energy Physics, Protvino*
[18]*Institute for Theoretical and Experimental Physics, Moscow*
[19]*J. Stefan Institute, Ljubljana*
[20]*Kanagawa University, Yokohama*
[21]*Institut für Experimentelle Kernphysik, Karlsruher Institut für Technologie, Karlsruhe*
[22]*Korea Institute of Science and Technology Information, Daejeon*
[23]*Korea University, Seoul*
[24]*Kyungpook National University, Taegu*
[25]*École Polytechnique Fédérale de Lausanne (EPFL), Lausanne*
[26]*Faculty of Mathematics and Physics, University of Ljubljana, Ljubljana*
[27]*Luther College, Decorah, Iowa 52101*
[28]*University of Maribor, Maribor*
[29]*Max-Planck-Institut für Physik, München*
[30]*University of Melbourne, School of Physics, Victoria 3010*
[31]*Graduate School of Science, Nagoya University, Nagoya*

 

[32]Kobayashi-Maskawa Institute, Nagoya University, Nagoya
[33]Nara Women's University, Nara
[34]National Central University, Chung-li
[35]National United University, Miao Li
[36]Department of Physics, National Taiwan University, Taipei
[37]H. Niewodniczanski Institute of Nuclear Physics, Krakow
[38]Nippon Dental University, Niigata
[39]Niigata University, Niigata
[40]University of Nova Gorica, Nova Gorica
[41]Osaka City University, Osaka
[42]Pacific Northwest National Laboratory, Richland, Washington 99352
[43]Panjab University, Chandigarh
[44]Research Center for Nuclear Physics, Osaka University, Osaka
[45]University of Science and Technology of China, Hefei
[46]Seoul National University, Seoul
[47]Sungkyunkwan University, Suwon
[48]School of Physics, University of Sydney, NSW 2006
[49]Tata Institute of Fundamental Research, Mumbai
[50]Excellence Cluster Universe, Technische Universität München, Garching
[51]Toho University, Funabashi
[52]Tohoku Gakuin University, Tagajo
[53]Tohoku University, Sendai
[54]Department of Physics, University of Tokyo, Tokyo
[55]Tokyo Institute of Technology, Tokyo
[56]Tokyo Metropolitan University, Tokyo
[57]Tokyo University of Agriculture and Technology, Tokyo
[58]CNP, Virginia Polytechnic Institute and State University, Blacksburg, Virginia 24061
[59]Yamagata University, Yamagata
[60]Yonsei University, Seoul

(Received 31 January 2012; published 3 May 2012)

We report first observations of $B_s^0 \to J/\psi\eta$ and $B_s^0 \to J/\psi\eta'$. The results are obtained from 121.4 fb$^{-1}$ of data collected at the $\Upsilon(5S)$ resonance with the Belle detector at the KEKB $e^+e^-$ collider. We obtain the branching fractions $\mathcal{B}(B_s^0 \to J/\psi\eta) = [5.10 \pm 0.50(\text{stat}) \pm 0.25(\text{syst})^{+1.14}_{-0.79}(N_{B_s^{(*)}\bar{B}_s^{(*)}})] \times 10^{-4}$, and $\mathcal{B}(B_s^0 \to J/\psi\eta') = [3.71 \pm 0.61(\text{stat}) \pm 0.18(\text{syst})^{+0.83}_{-0.57}(N_{B_s^{(*)}\bar{B}_s^{(*)}})] \times 10^{-4}$. The ratio of the two branching fractions is measured to be $\frac{\mathcal{B}(B_s \to J/\psi\eta')}{\mathcal{B}(B_s \to J/\psi\eta)} = 0.73 \pm 0.14(\text{stat}) \pm 0.02(\text{syst})$.

DOI: 10.1103/PhysRevLett.108.181808 PACS numbers: 13.25.Hw, 14.40.Nd

The decays $B_s^0 \to J/\psi\eta^{(\prime)}$ are dominated by the $b \to c\bar{c}s$ process shown in Fig. 1. The $J/\psi\eta^{(\prime)}$ final states are $CP$-even eigenstates; their time distributions can be used to directly measure the $B_s^0$ width difference $\Delta\Gamma_s$ and the $CP$-violating phase $\phi_s$ [1] without an angular analysis. Assuming flavor SU(3) symmetry and factorization, the $B_s^0 \to J/\psi\eta^{(\prime)}$ branching fractions relative to the decay $B_d^0 \to J/\psi K^0$ are estimated to be [2]

$$\frac{\mathcal{B}(B_s^0 \to J/\psi\eta^{(\prime)})}{\mathcal{B}(B_d^0 \to J/\psi K^0)} = \sin^2\phi_P(\cos^2\phi_P) \times p^{*3}_{B_s^0}/p^{*3}_{B_d^0},$$

where $p^*$ is the momentum of $J/\psi$ in the rest frame of the $B_s^0$ or $B_d^0$. Here $\phi_P = (41.4 \pm 0.5)^\circ$ [3] is the pseudoscalar mixing angle in the flavor basis with $\eta(\prime) = \frac{1}{\sqrt{2}}[u\bar{u} + d\bar{d}]\cos\phi_P(\sin\phi_P) - (+)s\bar{s}\sin\phi_P(\cos\phi_P)$, and other possible flavor singlet content of the $\eta'$ such as gluonium is neglected. Using this relation and the value $\mathcal{B}(B_d^0 \to J/\psi K^0) = 8.71 \times 10^{-4}$ [4], we expect $\mathcal{B}(B_s^0 \to J/\psi\eta^{(\prime)}) \sim 4.16(4.31) \times 10^{-4}$. The ratio of the two branching fractions $\mathcal{B}(B_s^0 \to J/\psi\eta')/\mathcal{B}(B_s^0 \to J/\psi\eta)$ is expected to be $1.04 \pm 0.04$. This ratio estimation does not require flavor SU(3) or the assumption of factorization [5] and can be used to test the $\eta - \eta'$ mixing scheme [5,6]. The only previous experimental result for these decay channels is the 90% confidence level upper limit $\mathcal{B}(B_s^0 \to J/\psi\eta) < 3.8 \times 10^{-3}$ [7].

In this Letter, we report measurements of fully reconstructed $B_s^0 \to J/\psi\eta$ and $B_s^0 \to J/\psi\eta'$ decays using a 121.4 fb$^{-1}$ data sample collected with the Belle detector

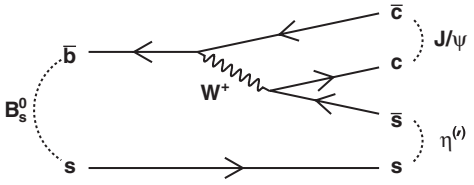


FIG. 1. Dominant diagram for the processes $B_s^0 \to J/\psi\eta^{(\prime)}$.

at the KEKB asymmetric-energy $e^+e^-$ collider [8] operated at the $\Upsilon(5S)$ resonance. $B_s^0$ mesons can be produced in three $\Upsilon(5S)$ decays: $\Upsilon(5S) \to B_s^* \bar{B}_s^*$, $B_s^* \bar{B}_s^0$, and $B_s^0 \bar{B}_s^0$ where the $B_s^*$ mesons decay to $B_s^0\gamma$. The number of $B_s^{(*)}\bar{B}_s^{(*)}$ pairs in the sample is measured to be $N_{B_s^{(*)}\bar{B}_s^{(*)}} = (7.1 \pm 1.3) \times 10^6$ using inclusive $D_s$ production methods described in Refs. [9,10]. The fractions of $B_s^0$ production channels are defined as $f_{B_s^*\bar{B}_s^*} = N_{B_s^*\bar{B}_s^*}/N_{B_s^{(*)}\bar{B}_s^{(*)}}$, $f_{B_s^*\bar{B}_s^0} = N_{B_s^*\bar{B}_s^0}/N_{B_s^{(*)}\bar{B}_s^{(*)}}$.

The Belle detector is a large-solid-angle magnetic spectrometer that consists of a silicon vertex detector, a 50-layer central drift chamber (CDC), an array of aerogel threshold Cherenkov counters (ACC), a barrel-like arrangement of time-of-flight scintillation counters, and an electromagnetic calorimeter (ECL) comprised of CsI(Tl) crystals located inside a superconducting solenoid coil that provides a 1.5 T magnetic field. An iron flux return located outside the coil is instrumented to detect $K_L^0$ mesons and identify muons. The detector is described in detail elsewhere [11].

Charged tracks are required to originate within 0.5 cm in the radial direction and within 5 cm in the beam direction, with respect to the interaction point. Electron candidates are identified by combining information from the ECL, the CDC ($dE/dx$), and the ACC. Muon candidates are identified through track penetration depth and hit patterns in the $K_L^0$ muon system. The identification of pions is based on combining information from the CDC ($dE/dx$), the time-of-flight scintillation counters, and the ACC.

Pairs of oppositely charged leptons $l^+l^-$ ($l = e$ or $\mu$) and bremsstrahlung photons lying within 50 mrad of $e^+$ or $e^-$ tracks are combined to form $J/\psi$ meson candidates. The leptons are required to be positively identified as electrons or muons and the dilepton invariant mass is required to lie in the ranges $-150\ \mathrm{MeV}/c^2 < M_{ee(\gamma)} - m_{J/\psi} < 36\ \mathrm{MeV}/c^2$ and $-60\ \mathrm{MeV}/c^2 < M_{\mu\mu} - m_{J/\psi} < 36\ \mathrm{MeV}/c^2$, where $m_{J/\psi}$ denotes the nominal $J/\psi$ mass [4], and $M_{ee(\gamma)}$ and $M_{\mu\mu}$ are the reconstructed invariant masses for $e^+e^-(\gamma)$ and $\mu^+\mu^-$, respectively.

Photon candidates are selected from ECL showers that are not associated with charged tracks. An energy deposition with a photonlike shower shape and an energy greater than 50 MeV is required. Candidate $\pi^0 \to \gamma\gamma$ decays are selected by combining two photon candidates with an invariant mass in the range $115\ \mathrm{MeV}/c^2 < M_{\gamma\gamma} < 155\ \mathrm{MeV}/c^2$.

Candidate $\eta$ mesons are reconstructed in the $\gamma\gamma$ and $\pi^+\pi^-\pi^0$ final states. We require the invariant mass to be in the range $500\ \mathrm{MeV}/c^2 < M_{\gamma\gamma} < 575\ \mathrm{MeV}/c^2([-3.5\sigma, 2.0\sigma])$ and $535\ \mathrm{MeV}/c^2 < M_{\pi^+\pi^-\pi^0} < 560\ \mathrm{MeV}/c^2(\pm 2.5\sigma)$.

Candidate $\eta'$ mesons are reconstructed in the $\eta\pi^+\pi^-$ and $\rho^0\gamma$ channels. Since $\eta$ candidates are selected in two channels, there are three subchannels for $\eta'$ reconstruction. Candidate $\rho^0 \to \pi^+\pi^-$ decays are oppositely charged pion pairs satisfying $550\,\mathrm{MeV}/c^2 < M_{\pi^+\pi^-} < 900\,\mathrm{MeV}/c^2$ and a helicity angle requirement $|\cos\theta_{\mathrm{hel}}| < 0.85$ since the $\rho^0$ in $\eta' \to \rho^0\gamma$ is longitudinally polarized. Here $\theta_{\mathrm{hel}}$ is the helicity angle of $\rho^0$, calculated as the angle between the direction of the $\pi^+$ and the direction opposite to the $\eta'$ momentum in the $\rho^0$ rest frame. We require the reconstructed $\eta'$ invariant mass to satisfy $940\ \mathrm{MeV}/c^2 < M_{\eta'} < 975\ \mathrm{MeV}/c^2(\pm 3\sigma)$.

We combine $J/\psi$ and $\eta^{(\prime)}$ candidates to form $B_s^0$ mesons. Signal candidates are identified by two kinematic variables computed in the $\Upsilon(5S)$ rest frame: the energy difference $\Delta E = E_B^* - E_{\mathrm{beam}}$ and the beam-energy constrained mass $M_{\mathrm{bc}} = \sqrt{(E_{\mathrm{beam}})^2 - (p_B^*)^2}$, where $E_B^*$ and $p_B^*$ are the energy and momentum of the reconstructed $B_s^0$ candidate. To improve the $\Delta E$ and $M_{\mathrm{bc}}$ resolutions, mass-constrained kinematic fits are applied to $J/\psi$, $\pi^0$, and $\eta^{(\prime)}$ candidates. We retain $B_s^0$ meson candidates with $|\Delta E| < 0.4$ GeV and $M_{\mathrm{bc}} > 5.25\ \mathrm{GeV}/c^2$ for further analysis. The candidate that has a minimum sum of $\chi^2$'s for the mass-constrained fits is selected if there is more than one candidate.

The background is dominated by two-jet-like continuum events of the type $e^+e^- \to q\bar{q}(q = u, d, s, c)$, together with other $B$ meson decay modes ($B = B_s^0$, $B_d^0$, $B^\pm$). To suppress the continuum background, we require the ratio of second to zeroth Fox-Wolfram moments [12] to be less than 0.4. This requirement is optimized by maximizing a figure of merit $N_S/\sqrt{N_S + N_B}$, where $N_S$ is the expected number of signal events and $N_B$ is the number of background events estimated from Monte Carlo simulation, in the $B_s^*\bar{B}_s^*$ signal region.

Signal and background distributions in $\Delta E$ and $M_{\mathrm{bc}}$ after all selections are parametrized separately for each $B_s^0 \to J/\psi\eta^{(\prime)}$ subchannel. The signal shapes for the two $\eta$ (three $\eta'$) subchannels are described with a Crystal Ball function [13] (the sum of a Crystal Ball and a Gaussian function) in $\Delta E$ and a Crystal Ball function in $M_{\mathrm{bc}}$. The means and widths of the distributions are calibrated with respect to Monte Carlo values using a control sample of $B^+ \to J/\psi K^{*+}(K^{*+} \to K^+\pi^0)$ decays collected at the $\Upsilon(4S)$ resonance. The background shapes for all $\eta^{(\prime)}$ subchannels are smooth and described with an exponential function in $\Delta E$ and an ARGUS function [14] in $M_{\mathrm{bc}}$.

An unbinned, extended maximum likelihood fit is performed simultaneously to the total five two-dimensional $\Delta E - M_{\mathrm{bc}}$ distributions. The branching fraction of each signal mode is a common parameter shared among the corresponding $\eta^{(\prime)}$ subchannels. The parameters $f_{B_s^*\bar{B}_s^*}$ and $f_{B_s^*\bar{B}_s^0}$ are also common to all five subchannels.

In the fit, the total probability density function consists of a signal and background component. The signal component includes contributions from the three $B_s^0$ pair production channels. The signal normalization for the $B_s^*\bar{B}_s^*$

TABLE I. A summary of the product of the sub-branching fraction and efficiency for various subchannels. Here $\mathcal{B}_i = \mathcal{B}(J/\psi \to l^+l^-)\mathcal{B}(\eta^{(\prime)} \to \text{final state})$, with the $J/\psi$ decaying to $e^+e^-$ or $\mu^+\mu^-$.

| Subchannel | $\mathcal{B}_i\epsilon_i$ |
|---|---|
| $B_s^0 \to J/\psi\eta(\gamma\gamma)$ | 1.40% |
| $B_s^0 \to J/\psi\eta(\pi^+\pi^-\pi^0)$ | 0.55% |
| Total $B_s^0 \to J/\psi\eta$ | 1.95% |
| $B_s^0 \to J/\psi\eta'(\eta(\gamma\gamma)\pi^+\pi^-)$ | 0.45% |
| $B_s^0 \to J/\psi\eta'(\eta(3\pi)\pi^+\pi^-)$ | 0.22% |
| $B_s^0 \to J/\psi\eta'(\rho^0\gamma)$ | 0.96% |
| Total $B_s^0 \to J/\psi\eta'$ | 1.63% |

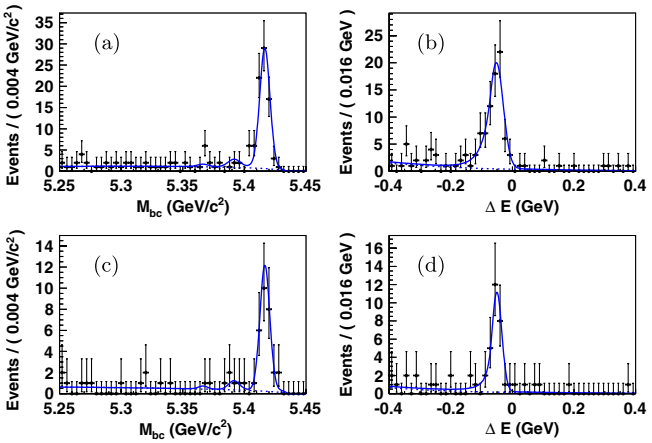


FIG. 2 (color online). $M_{\rm bc}$ and $\Delta E$ distributions for the $J/\psi\eta(\gamma\gamma)$ channel (a), (b) and the $J/\psi\eta(\pi^+\pi^-\pi^0)$ channel (c), (d). The projections are shown in the $B_s^*\bar{B}_s^*$ signal region with $\Delta E \in [-116, 12]$ MeV (a), (c), and with $M_{\rm bc} \in [5.405, 5.428]$ GeV/$c^2$ (b), (d). Solid curves show projections of fit results. Backgrounds are represented by the blue dotted curves. Two small bumps around 5.37 and 5.39 GeV/$c^2$ in (a), (c) are contributions from $B_s^0\bar{B}_s^0$ and $B_s^*\bar{B}_s^0$ production channels, due to the overlap of the $\Delta E$ signal regions.

production channel is parametrized as $N_{\rm sig} = 2 \times N_{B_s^{(*)}\bar{B}_s^{(*)}} f_{B_s^*\bar{B}_s^*} \mathcal{B}(B_s^0 \to J/\psi\eta^{(\prime)})\mathcal{B}_i\epsilon_i$ for each $\eta^{(\prime)}$ subchannel $i$. The product $\mathcal{B}_i = \mathcal{B}(J/\psi \to l^+l^-)\mathcal{B}_i(\eta^{(\prime)})$ is the total branching fraction for a $J/\psi$ and an $\eta^{(\prime)}$ decaying to the reconstructed final states [4], and $\epsilon_i$ is the reconstruction efficiency obtained from Monte Carlo simulation. The values of the weighted efficiencies $\mathcal{B}_i\epsilon_i$ are listed in Table I. The signal yields in the $B_s^*\bar{B}_s^0$ and $B_s^0\bar{B}_s^0$ production channels are obtained in a similar manner, with $f_{B_s^*\bar{B}_s^*}$ replaced by $f_{B_s^*\bar{B}_s^0}$ and $f_{B_s^0\bar{B}_s^0} = 1 - f_{B_s^*\bar{B}_s^*} - f_{B_s^*\bar{B}_s^0}$, respectively. The floating parameters in the fit are the branching fractions $\mathcal{B}(B_s^0 \to J/\psi\eta^{(\prime)})$, $f_{B_s^*\bar{B}_s^*}$, $f_{B_s^*\bar{B}_s^0}$, and the corresponding background yields and shapes for different $\eta^{(\prime)}$ subchannels. This fit procedure was checked with six fully simulated Monte Carlo samples that included both signal and background, each normalized to the data luminosity. The results show that the fitted branching fractions for both modes recover the input values.

The projections of the fit to the 121.4 fb$^{-1}$ data sample in the $B_s^*\bar{B}_s^*$ signal region are shown in Figs. 2 and 3. There are good agreements between fit curve and data points in all subchannels' projections. We obtain a total of $141 \pm 14$ $B_s^0 \to J/\psi\eta$ events with a statistical significance of $21.9\sigma$ and $86 \pm 14$ $B_s^0 \to J/\psi\eta'$ events with a statistical significance of $10.3\sigma$ in all three $\Upsilon(5S) \to B_s^{(*)}\bar{B}_s^{(*)}$ channels. The statistical significances are calculated as $\sqrt{2\ln(L_{\rm max}/L_0)}$, where $L_{\rm max}$ and $L_0$ are the maximum likelihood values, while the corresponding signal yield is set to zero for $L_0$. The $B_s^0 \to J/\psi\eta$ and $B_s^0 \to J/\psi\eta'$ decays are observed for the first time. The $B_s^0$ pair production fractions are measured to be $f_{B_s^*\bar{B}_s^*} = (90.5 \pm 3.2 \pm 0.1)\%$, $f_{B_s^*\bar{B}_s^0} = (4.9 \pm 2.5 \pm 0.0)\%$, with a correlation coefficient $(-0.72)$. This result is consistent with the value $f_{B_s^*\bar{B}_s^*} = (87.0 \pm 1.7)\%$ [15] obtained from 121.4 fb$^{-1}$ of data using the $B_s^0 \to D_s^-\pi^+$ reconstruction method described in Ref. [16].

The systematic uncertainties due to the signal function mean and width are determined by varying each parameter by its error from the control sample calibration, repeating the fit, and summing the shifts in the branching fraction in quadrature. The lepton and pion identification efficiencies from Monte Carlo calculations are calibrated using $\gamma\gamma \to l^+l^-$ and $D^{*+} \to D^0\pi^+(D^0 \to K^-\pi^+)$ control samples in data, respectively. Systematic errors for branching fractions are summarized in Table II. Those on $f_{B_s^*\bar{B}_s^*}$ and $f_{B_s^*\bar{B}_s^0}$ are dominated by the signal shape uncertainty. The large systematic error due to $N_{B_s^{(*)}\bar{B}_s^{(*)}}$ is quoted separately in the final results.

The ratio of the two branching fractions is also determined, where the systematic error due to $N_{B_s^{(*)}\bar{B}_s^{(*)}}$ cancels. For this, the statistical errors of the two modes are combined using error propagation. Correlated systematic errors due to calibration, track reconstruction, and particle identification are determined by varying the numerator and denominator simultaneously. Other systematic sources are treated independently.

TABLE II. Relative systematic errors (in %) for $\mathcal{B}(J/\psi\eta^{(\prime)})$.

| Source | $\mathcal{B}(J/\psi\eta)$ | $\mathcal{B}(J/\psi\eta')$ |
|---|---|---|
| Signal shape calibration | $+0.4, -0.5$ | $+1.1, -1.3$ |
| Track reconstruction | 0.8 | 1.4 |
| Electron identification | 1.5 | 1.5 |
| Muon identification | 1.8 | 1.7 |
| Pion identification | 0.5 | 2.1 |
| $\eta(\pi^0) \to \gamma\gamma$ selection | 4.0 | 2.8 |
| $\mathcal{B}(J/\psi \to ll)$ | 0.7 | 0.7 |
| $\mathcal{B}(\eta^{(\prime)} \to \text{final states})$ | 0.5 | 1.2 |
| Total [without $N_{B_s^{(*)}\bar{B}_s^{(*)}}$] | 4.8 | 4.8 |
| $N_{B_s^{(*)}\bar{B}_s^{(*)}}$ | $+22.4, -15.5$ | |

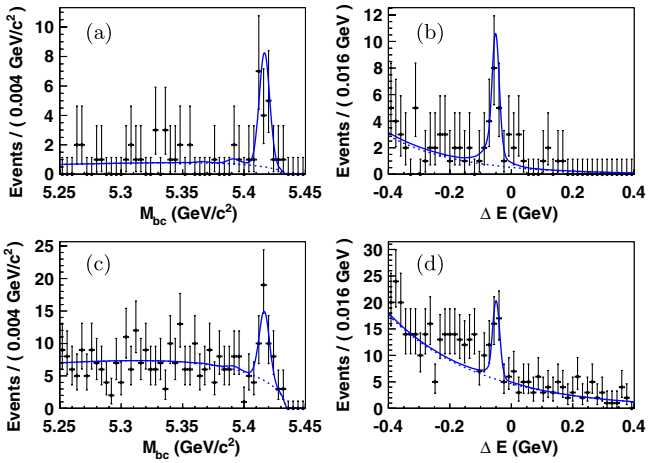


FIG. 3 (color online). Fit projections for the clean $J/\psi\eta'(\eta\pi^+\pi^-)$ channel with two $\eta$ subchannels combined (a), (b) and the $J/\psi\eta'(\rho^0\gamma)$ channel (c), (d). The projections are shown in the $B_s^*\bar{B}_s^*$ signal region with $\Delta E \in [-87, -15]$ MeV (a), (c), and with $M_{\rm bc} \in [5.405, 5.429]$ GeV/$c^2$ (b), (d). The sum of all backgrounds is represented by the blue dotted curves.

In summary, we observe $B_s^0 \to J/\psi\eta$ and $B_s^0 \to J/\psi\eta'$ decays for the first time with significances over $10\sigma$ by taking advantage of the low background $e^+e^-$ environment at Belle. We measure the branching fractions

$$\mathcal{B}(B_s^0 \to J/\psi\eta) = [5.10 \pm 0.50(\text{stat}) \pm 0.25(\text{syst})^{+1.14}_{-0.79}(N_{B_s^{(*)}\bar{B}_s^{(*)}})] \times 10^{-4},$$

$$\mathcal{B}(B_s^0 \to J/\psi\eta') = [3.71 \pm 0.61(\text{stat}) \pm 0.18(\text{syst})^{+0.83}_{-0.57}(N_{B_s^{(*)}\bar{B}_s^{(*)}})] \times 10^{-4}.$$

These branching fractions are consistent with SU(3) expectations using the measured value of $\mathcal{B}(B_d^0 \to J/\psi K^0)$ [2]. The ratio of the two branching fractions is measured to be $\frac{\mathcal{B}(B_s \to J/\psi\eta')}{\mathcal{B}(B_s \to J/\psi\eta)} = 0.73 \pm 0.14(\text{stat}) \pm 0.02(\text{syst})$. This ratio is smaller than the expected value of $1.04 \pm 0.04$ at the $2.1\sigma$ level; a significant deviation would indicate additional flavor singlet components in the $\eta'$ other than $u\bar{u}$, $d\bar{d}$, $s\bar{s}$ pairs or violation of the $\eta - \eta'$ mixing scheme.

We thank the KEKB group for excellent operation of the accelerator, the KEK cryogenics group for efficient solenoid operations, and the KEK computer group and the NII for valuable computing and SINET4 network support. We acknowledge support from MEXT, JSPS and Nagoya's TLPRC (Japan); ARC and DIISR (Australia); NSFC (China); MSMT (Czechia); DST (India); INFN (Italy); MEST, NRF, NSDC of KISTI, and WCU (Korea); MNiSW (Poland); MES and RFAAE (Russia); ARRS (Slovenia); SNSF (Switzerland); NSC and MOE (Taiwan); and DOE and NSF (U.S.). J. Li acknowledges support from WCU Grant No. R32-10155.

[1] I. Dunietz, R. Fleischer, and U. Nierste, Phys. Rev. D **63**, 114015 (2001).
[2] P. Z. Skands, J. High Energy Phys. 01 (2001) 008; P. Colangelo, F. De Fazio, and W. Wang, Phys. Rev. D **83**, 094027 (2011).
[3] F. Ambrosino *et al.* (KLOE Collaboration), J. High Energy Phys. 07 (2009) 105.
[4] K. Nakamura *et al.* (Particle Data Group), J. Phys. G **37**, 075021 (2010).
[5] R. Fleischer, R. Knegjens, and G. Ricciardi, Eur. Phys. J. C **71**, 1798 (2011).
[6] C. E. Thomas, J. High Energy Phys. 10 (2007) 026.
[7] M. Acciarri *et al.* (L3 Collaboration), Phys. Lett. B **391**, 481 (1997).
[8] S. Kurokawa and E. Kikutani, Nucl. Instrum. Methods Phys. Res., Sect. A **499**, 1 (2003), and other papers included in this volume.
[9] M. Artuso *et al.* (CLEO Collaboration), Phys. Rev. Lett. **95**, 261801 (2005).
[10] A. Drutskoy *et al.* (Belle Collaboration), Phys. Rev. Lett. **98**, 052001 (2007).
[11] A. Abashian *et al.* (Belle Collaboration), Nucl. Instrum. Methods Phys. Res., Sect. A **479**, 117 (2002).
[12] The Fox-Wolfram moments were introduced in G. C. Fox and S. Wolfram, Phys. Rev. Lett. **41**, 1581 (1978).
[13] T. Skwarnicki, Ph.D. thesis, Institute for Nuclear Physics, Krakow 1986 [Report DESY F31-86-02].
[14] H. Albrecht *et al.* (ARGUS Collaboration), Phys. Lett. B **185**, 218 (1987).
[15] J. Li *et al.* (Belle Collaboration), Phys. Rev. Lett. **106**, 121802 (2011).
[16] R. Louvot *et al.* (Belle Collaboration), Phys. Rev. Lett. **102**, 021801 (2009).